Journal of Institute of Science and Technology, 30(1), 73-81 (2025)
ISSN: 2467-9062 (print), e-ISSN: 2467-9240
https://doi.org/10.3126/jist.v30i1.68879

Research Article

WATER ADSORPTION ON PRISTINE AND VACANCY DEFECTED h-BN MONOLAYER: FIRST-PRINCIPLES STUDY

Santosh Aryal, Ganesh Paudel, Madhav Nepal, Dipak Oli, Om Shree Rijal, Hari Krishna Neupane*
Amrit Campus, Institute of Science and Technology, Tribhuvan University, Kathmandu, Nepal
**Correspondence: hari.neupane@ac.tu.edu.np*

(Received:** August 18, 2024; **Final Revision:** March 01, 2025; **Accepted:** March 03, 2025**)

ABSTRACT
The adsorption of liquid or gas molecules on pristine or structurally defective systems exhibits unique properties. They have budding uses in the field of device applications. So, in this work, we have studied the structural, electronic, and magnetic properties of water adsorbed h-BN (w-hBN), and water adsorption on: 1B atom vacancy defect in h-BN (w-1B-hBN), 1N atom vacancy defect in h-BN (w-1N-hBN), nearest neighbours of 1B &1N atoms vacancies defect in h-BN (w-nBN-hBN), and alternate zone of 1B &1N atoms vacancies defect in h-BN (w-aBN-hBN), monolayer supercell structures using density functional theory (DFT) method by employing Quantum ESPRESSO computational tool. For the structural properties, we have estimated the bond length between B & N atoms, and ground state energy of materials. They are found to be compact form of stable two-dimensional materials. Material's compactness is increased by decreasing number of vacancy defects in the material. Electronic properties of considered materials are studied by the analysis of their band structure and density of states (DOS) calculations. It is found that w-1B-hBN is a p-type semiconductor, and w-hBN, w-1B-hBN, w-1N-hBN, w-nBN-hBN, w-aBN-hBN are n-type semiconductors. Magnetic properties of considered materials are examined from their DOS and partial density of states (PDOS) plots, it is found that w-hBN is non-magnetic material, and w-1B-hBN, w-1N-hBN, w-nBN-hBN & w-aBN-hBN are magnetic materials. Magnetic properties are generated due to the arrangement of unpaired up or down spin states of electrons in the individual orbitals of atoms present in the materials.

Keywords: DFT, monolayer, orbitals, spin states, supercell

INTRODUCTION
Exploring of two-dimensional (2D) materials (Novoselov *et al.,* 2016) were not in highlight among the young researcher till 2003. Nonetheless, with the successful synthesis of graphene in 2004 (Xu, *et al.,* 2013; Uddin *et al.,* 2023), there has been a great deal of interest in the study of 2D materials. By considering the numerous uses, 2D materials are extensively researched (Butler *et al.,* 2013; Bhimanapati *et al.,* 2015). Their unique mechanical, optical, electronic, and gas sensing properties could be crucial components in advanced optoelectronic and electronic applications (Butler *et al.,* 2013; Zhang *et al.,* 2016). Among various 2D materials, hexagonal boron nitride (h-BN) is one of the highly researched materials as it is thermally and chemically stable under a variety of circumstances (Neupane & Adhikari, 2021a; He *et al.,* 2022). The Boron (B) and Nitrogen (N) atom stoichiometry ratio of the honeycomb structure of h-BN is 1:1, and they are arranged in a honeycomb lattice within each layer. Due to various bonding configurations between B and N atoms, boron nitride (BN) can take four polymorphic forms: wurtzite (w-BN), rhombohedral (r-BN), cubic (c-BN), and hexagonal (h-BN). The various characteristics of BN materials are significantly influenced by the crystal structures of these forms. The most stable hexagonal form of graphite is h-BN, and it functions as an insulator. The differing energies of B & N atoms, however, cause a considerable difference in the band structures of h-BN and graphite; as a result, h-BN has a wide bandgap energy of value (~ 4.96 eV), and a slight lattice misfit with graphite 1.8% (Pierucci *et al.,* 2018; Neupane & Adhikari, 2021a). Moreover, h-BN has good mechanical, optical, electronic, and thermal properties. Hence, it is a desirable material that can be used in the field of devices application. Scientists have added (adsorbed) or removed (create vacancy defect) the atoms in or from the structure of material for the investigation of their novelty properties (Mali *et al.,* 2015; Ren *et al.,* 2021). The fundamental characteristics of the material were tuned by the suitable doping of the foreign elements and the creation of vacancies in the compound (Zhang & Zhang, 2010; Patra *et al.,* 2018; Oli, 2024). The deliberate removal of one atom from the system in order to introduce or exacerbate other foreign elements is known as a vacancy defect. Adsorption is a method of covering a material's surface with a thin layer that can be carried out in two ways: chemically or physically. Adsorption is referred to as chemical adsorption if the adsorbed molecule is chemically bound; otherwise, it is referred to as physical adsorption.

As far as we know, no study has been made to study the structural, electronic, and magnetic properties of water adsorption on: monolayer (4×4) supercell

structure of h-BN (w-hBN), 1B atom vacancy defect in h-BN (w-1B-hBN), 1N atom vacancy defect in h-BN (w-1N-hBN), nearest neighbors of 1B &1N atom vacancies defect in h-BN (w-nBN-hBN), and alternate zone of 1B &1N atom vacancies defect in h-BN (w-aBN-hBN). We thought that these materials would have novel properties than previously researched BN based materials. After tuned unique (novel) properties in the materials, they can be used in the field of devices application. In the present work, we have investigated the structural, electronic, and magnetic properties of w-hBN, w-1B-hBN, w-1N-hBN, w-nBN-hBN & w-aBN-hBN materials using spin-polarized Density Functional Theory (DFT) method by employing Quantum ESPRESSO (QE) computational tool (Giannozzi *et al.,* 2009).

MATERIALS AND METHODS

In this section, we have explained details of computational methods and studied materials. We have investigated the structural, electronic, and magnetic properties of water adsorbed (4×4) supercell structure of h-BN monolayer (w-hBN), and water adsorbed 1B vacancy defect h-BN (w-1B-hBN), 1N vacancy defect h-BN (w-1N-hBN), nearest neighbors 1B & 1N vacancies defect h-BN (w-nBN-hBN), and alternate region of 1B & 1N vacancies defect h-BN (w-aBN-hBN), materials by using density functional theory (DFT) (Kohn & Sham, 1965) method under Quantum ESPRESSO (QE) (Giannozzi *et al.,* 2009) as a computational tool. We have used Generalized Gradient Approximation (GGA) on the basis of PBE functional, for the calculations of exchange-correlation (XC) functional [Perdew *et al.,* 1996]. The ultra-soft pseudopotential (USPPs) (Kresse & Joubert, 1999), and plane wave basis set are used to examine the interaction of valence electrons of atoms in the system. For the structural optimization and relaxation, Broaden-Fletcher-Goldfarb-Shanno (BFGS) algorithm (Head & Zerner, 1985) is used. The calculations are continued until the change in total energy in between two consecutive self-consistent fields (scf) is found to be less than 10^{-4} Ry value, and force on each atom is obtained below 10^{-3} Ry/Bohr values. Marzarri-Vanderbilt (M-V) smearing method (Marzari *et al.,* 1999) is used for smearing by taking narrow broadening width of value 0.001 Ry. David diagonalization method is used in the self-consistency process, by taking mixing factor of defaults value 0.6. For the calculations fine band structure and density of states (DOS) plots, 200 k-points are taken along with the high symmetry points in the reciprocal lattice.

We have constructed the stable unit cell structure of hexagonal boron nitride (h-BN) by taking the optimized value of lattice parameter, kinetic energy cutoff, and k-points in the input file. (4×4) supercell structure of h-BN is obtained by extending the unit cell four-times along x-direction, and four-times along y-direction. Water molecules are adsorbed on that supercell cell structure of h-BN at a 3.24 Å distance from the surface of h-BN layer, and then relax calculations are done by using BFGS scheme. A stable relaxed structure of water adsorbed h-BN (w-hBN) is prepared. As we know, (4×4) supercell structure of h-BN monolayer consists of 32 (16-Boron & 16-Nitrogen) atoms. Single vacancy is created by randomly removing either 1B atom or 1N atom from h-BN structure of defect concentration value 0.03125 %, and two atoms (alternate zone of 1B & 1N atoms, or nearest neighbors 1B & 1N atoms) vacancies defect from h-BN structure of defect concentration value 0.0625%. These values are comparable value with other defective systems (Neupane, & Adhikari, 2020, Nepal, *et al.,* 2024). Hence, considered defected systems are suitable for the study of their structural, electronic and magnetic properties. Optimization and relax calculations of defected systems are done by using BFGS approach and found that they are stable materials. Additionally, water molecules are absorbed on these defective systems, by taking water molecules at various positions at 3.24 Å above the surface of defected surface of h-BN. Water adsorbed defected systems are then optimized and relax by using BFGS scheme. They are used to investigate the structural, electronic and magnetic properties by obtaining their band structure, density of states (DOS) and partial density of states (PDOS) plots. For the band structure calculations, a mesh of (6×6×1) k-points are used, while for the DOS & PDOS calculations, dense mesh of (16×16×1) k-point are employed for the self-consistent field (scf) calculations. For the structural visualization XCrySDen (Kokalj, 2003), and plotting purpose XmGrace (Turner, 2005) programs are used.

RESULTS AND DISCUSSION

In this section, firstly we have analyzed the structural properties of the materials considered. After that, we have determined their electronic and magnetic properties on the basis of band structures, DOS and PDOS plots. We have compared our findings with the reported values. Finally, we have drawn conclusions based on the found results.

Structural Properties

The structural properties of w-hBN, w-1B-hBN, w-1N-hBN, w-nBN-hBN, & w-aBN-hBN materials are examined by calculating their bond length between any two atoms, bond angle between three atoms, minimum ground state energy, and water adsorption energy. Firstly, we have prepared the stable (4×4) supercell structure of h-BN by extending a unit cell along x-and y-axis. That structure is optimized and determined its lattice parameter (a) of value 2.49 Å, kinetic energy cutoff (ecutoff) of value 35 Ry, charge density (ecutrho) of value 350 Ry, and k-point value (12×12×1). The ecutrho value is taken 350 Ry because for the uses of USPPs, ecutrho value is 10 times greater than ecutoff value. Water molecules are adsorbed on the various positions above the surface of h-BN, and then relax calculation is done. It is found that water is situated at 3.25 Å distance above the middle surface of h-BN,

which is more stable material than other configurations. We have estimated the bond length between B-N or N-B atoms before water adsorption, and after water adsorption on h-BN, they are found to be 1.42 Å &1.43 Å respectively. They fairly agree with the reported values (Liu *et al.,* 2014; Paudel *et al.,* 2023). It is seen that the structure is slightly expanded due to the adsorption of water molecules on h-BN. The bond angle between B-N-B or N-B-N atoms in the material are estimated and found to be 120^0. It means, there is no effect on bond angle by adsorbed water molecule. We have also calculated the minimum ground state energy of w-hBN, and found it to be -462 Ry. Hence, it is a stable material, which is shown in Fig. 1(a).

Moreover, we have prepared w-1B-hBN, w-1N-hBN, w-nBN-hBN, & w-aBN-hBN materials by adsorbing water molecules on various positions of B & N sites defected h-BN materials. In all materials, adsorbed water molecules are located at 3.23 Å distance from the middle site of defected h-BN materials, which are shown in Fig. 1(b-e), respectively. They are more stable materials than other configurations, because ground states energy of these materials have lower value than other configurations.

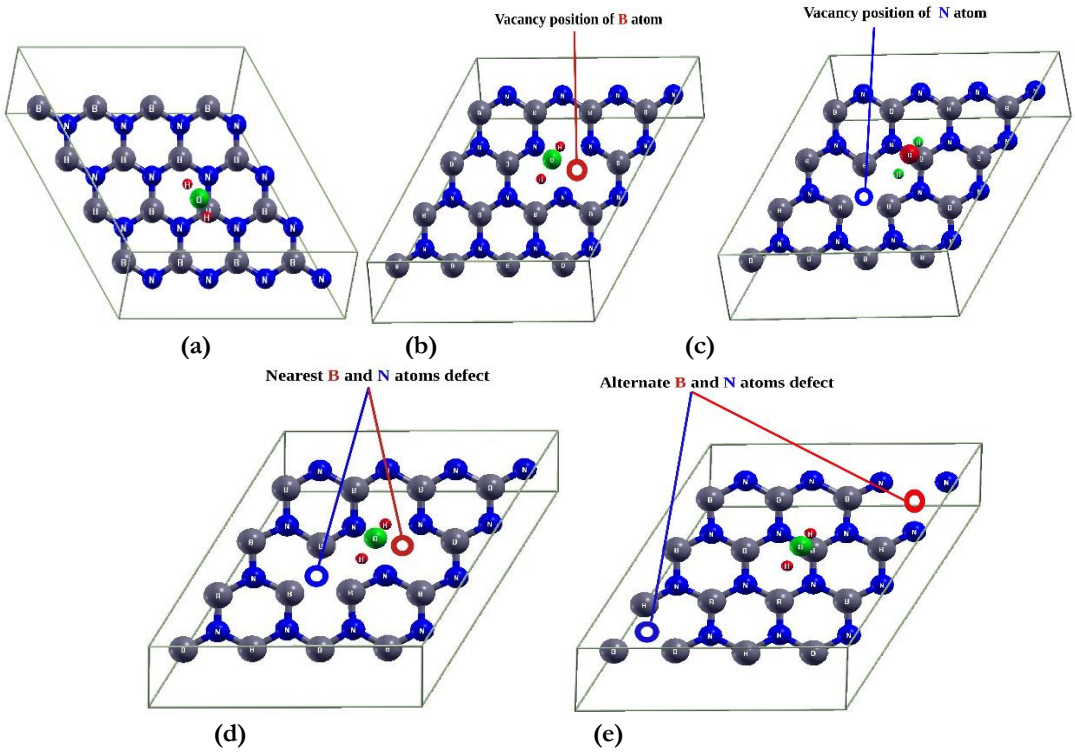

Figure 1. (Color online) Optimized and relax stable structures of water adsorption on pristine and vacancy defected h-BN material: (a) (4×4) supercell structure of w-hBN material, (b) (4×4) supercell structure of w-1B-hBN material, (c) (4×4) supercell structure of w-1N-hBN material, (d) (4×4) supercell structure of w-nBN-hBN material, and (e) (4×4) supercell structure of w-aBN-hBN material.

We have measured the bond length between B-N or N-B atoms in w-1B-hBN, w-1N-hBN, w-nBN-hBN, & w-aBN-hBN materials, and are found to be 1.45 Å, 1.45 Å, 1.47 Å & 1.48 Å respectively. They are closely with reported values (Liu *et al.,* 2014). From these calculations, we found that bond length of materials is increased by increasing its defect concentration, and hence water adsorbed on single vacancy defected materials are more compact than double vacancies defected materials. We also compared the bond length values in between water adsorption on h-BN, and B & N sites vacancy defected h-BN materials, it is found that water adsorbed h-BN material is more compact than water adsorbed defected h-BN materials. We have measured the bond angle between B-N-B or N-B-N atoms in above water adsorbed materials and found to be 120^0 of single vacancy defected structures while 118^0 of double defected structures. It means, water adsorbed on double vacancies defected material is slightly deformed. Moreover, we have estimated the minimum ground states energy of w-1B-hBN, w-1N-hBN, w-nBN-hBN, & w-aBN-hBN materials, and found to be -457.15 Ry, -455.09 Ry, -434.74 Ry, & -434.67 Ry respectively. These values are slightly higher than the minimum ground states energy of w-hBN material. It reveals that stability of w-1B-hBN, w-1N-hBN, w-nBN-hBN, & w-aBN-hBN materials are decreased as compared to w-hBN. It is also seen that stability of defected materials decreases by increasing in defect densities. Hence, stability of materials is arranged according to the following order w-hBN > w-1B-hBN > w-1N-hBN > w-nBN-hBN > w-aBN-hBN. We have estimated the water adsorption energies on w-hBN & w-1B-hBN, w-1N-hBN, w-nBN-hBN, & w-aBN-hBN

materials by using equation (1) & (2) (Vu *et al.,* 2020), respectively;

$$E_b = (E_w + E_{h\text{-}BN}) - E_{w\text{-}h\text{-}BN} \quad \ldots(1)$$

$$E_b = (E_w + E_{(h\text{-}BN)d}) - E_{(w\text{-}h\text{-}BN)d} \quad \ldots(2)$$

Where E_w, $E_{h\text{-}BN}$, $E_{w\text{-}h\text{-}BN}$, $E_{(h\text{-}BN)d}$ & $E_{(w\text{-}h\text{-}BN)d}$ denoted the ground state energy of: water molecule, h-BN, water adsorbed h-BN, vacancy defected h-BN, and water adsorbed vacancy defected h-BN materials respectively. The estimated water adsorption energies on w-hBN & w-1B-hBN, w-1N-hBN, w-nBN-hBN, & w-aBN-hBN materials are 1.62 eV, 1.64 eV, 1.63 eV, 1.58 eV & 1.59 eV respectively. These values are comparable with the values of other two-dimensional materials (Neupane & Adhikari, 2022). Water adsorption energy of double defective systems decreases than single defective systems, this is because atoms in water molecules are more interacted with the atoms in single defected systems. The calculated value of bond length, bond angles, water adsorption energy, minimum ground states energy of considered materials are given in Table 1.

Table 1. Estimated values of bond length between B-N or N-B atoms (b_l) Å, bond angle between B-N-B or N-B-N (b_a) degrees, distance between adsorbed water molecule with h-BN surface (d_w) Å, water adsorption energy (E_a) eV, and minimum ground states energy (E_g) Ry of w-hBN & w-1B-hBN, w-1N-hBN, w-nBN-hBN, & w-aBN-hBN materials.

Materials	(b_l) Å	$(b_a)^0$	(d_w) Å,	(E_g) Ry	(E_a) eV
w-hBN	1.43	120	3.25	-462.00	1.62
w-1B-hBN	1.45	120	3.23	-457.15	1.64
w-1N-hBN	1.45	120	3.23	-455.09	1.63
w-nBN-hBN	1.47	118	3.23	-434.74	1.58
w-aBN-hBN	1.48	118	3.23	-434.67	1.59

Electronic Properties

The nature of material can be predicted by the study of its electronic properties. Electronic properties of materials are determined by the analysis of their band structure and density of states (DOS) calculations. In the present work, we have investigated the electronic properties of w-hBN, w-1B-hBN, w-1N-hBN, w-nBN-hBN, & w-aBN-hBN materials on the basis of their band structures and DOS calculations. Band structure plots of considered materials are illustrated in Fig. 2(a-e), where highly symmetric points (Γ− *M* − *K* −Γ) are taken along the x-axis, and corresponding energies are taken along the y-axis. The horizontal dot line represents the Fermi energy level which separates the band regions, and vertical dot lines represent the highly symmetric points. For the calculation of fine band structure plot, we have used 200 k-points within the irreducible Brillouin zone (BZ).

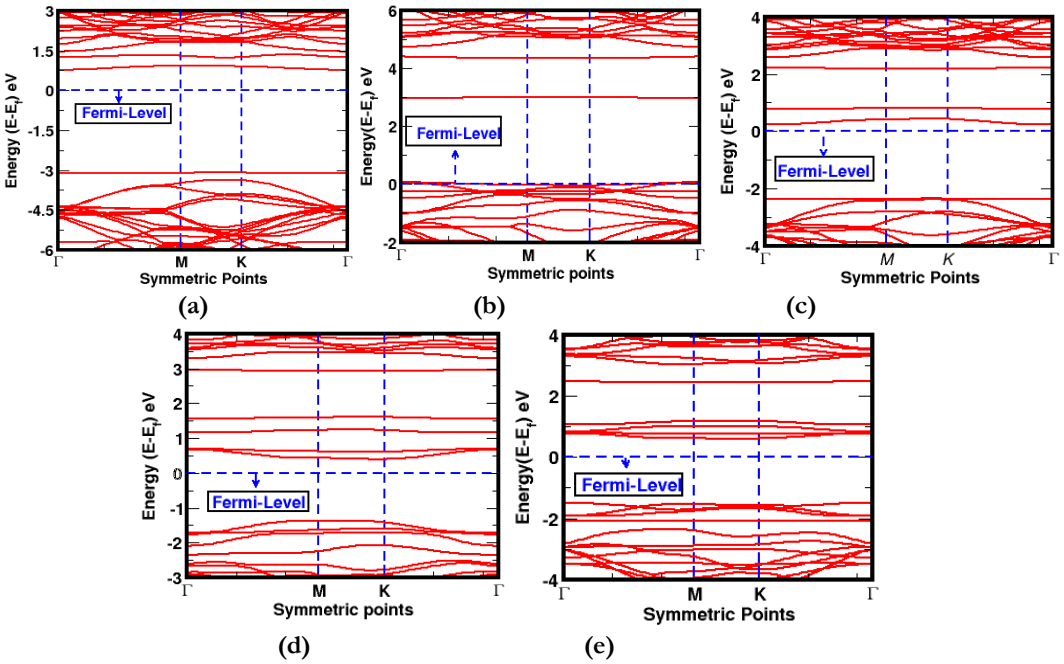

Figure 2. (Color online) Band structure of; (a) (4×4) supercell structure of w-hBN material, (b) (4×4) supercell structure of w-1B-hBN material, (c) (4×4) supercell structure of w-1N-hBN material, (d) (4×4) supercell structure of w-nBN-hBN material, and (e) (4×4) supercell structure of w-aBN-hBN material. The horizontal dot line represents the Fermi energy level, and vertical dot lines represent the high symmetric points.

We have determined the bandgap energies of w-hBN, w-1B-hBN, w-1N-hBN, w-nBN-hBN, & w-aBN-hBN materials which are found to be 3.96 eV, 2.89 eV, 2.72 eV, 2.04 eV & 1.30 eV respectively. They are estimated by the sum of distance between Fermi energy level to conduction band minimum (CBM), and Fermi energy level to valence band maximum (VBM). In w-hBN, distance from Fermi energy level to conduction band minimum, and Fermi energy level to valence band maximum are found to be 0.84 eV & 3.12 eV respectively. It is seen that the sum of these values gives 3.96 eV. Hence, it has semiconducting properties. From the estimation of energy gaps from Fermi energy level to CBM, and VBM, w-hBN has n-type Schottky barrier. Hence, it is an n-type semiconductor material. The band structure plot of w-hBN material is shown in Fig. 2(a). We have estimated the bandgap energy of w-1B-hBN material and found to be 2.89 eV. This energy is the sum of energy from Fermi energy level to CBM, and VBM. It is also found that distance from Fermi level to CBM is 2.89 eV, and Fermi level to VBM is 0 eV. It reflects that w-1B-hBN is a p-type semiconducting material, which is shown in Fig. 2(b). Similarly, we have estimated the bandgap energy of w-1N-hBN, and found to be 2.72 eV, which is the sum of the energy distance between Fermi energy level from CBM, and VBM. The distance from CBM to Fermi energy level is 0.36 eV, and distance from VBM to Fermi energy level is 2.36 eV. Hence, it is a n-type semiconducting material. Furthermore, we have estimated the bandgap energy of w-nBN-hBN & w-aBN-hBN materials. Bandgap energy of these materials is determined by the sum of the energy from CBM to Fermi energy level, and VBM to Fermi energy level, and are found to be 2.04 eV & 1.68 eV respectively. Band structure plots of these materials are shown in Fig. 2(d-e). The bandgap energy value 2.04 eV is obtained from the sum of 0.49 eV &1.55 eV values, which are obtained from the CBM to Fermi level & VBM to Fermi energy level respectively. Thus, w-nBN-hBN is a n-type semiconductor. Bandgap energy of w-aBN-hBN is 2.30 eV. This is the sum of energy from CBM to Fermi energy level (0.86 eV), and from VBM to Fermi energy level (1.50 eV). Thus, w-aBN-hBN has also n-type semiconducting nature. We have compared the bandgap energy of water adsorbed on B & N sites vacancy defected h-BN materials with the bandgap energy of water adsorption on pristine h-BN monolayer material. It is found that bandgap energy decreases on water adsorption defected materials (Neupane & Adhikari, 2021). Therefore, bandgap energy is affected by adsorbed water molecules on defected h-BN materials. Narrow bandgap energy materials have potential applications in the fields of devices. Additionally, we have estimated the bandgap energy of w-hBN, w-1B-hBN, w-1N-hBN, w-nBN-hBN, & w-aBN-hBN materials on the basis of their DOS plots, they are shown in Fig. 3(a-e), respectively.

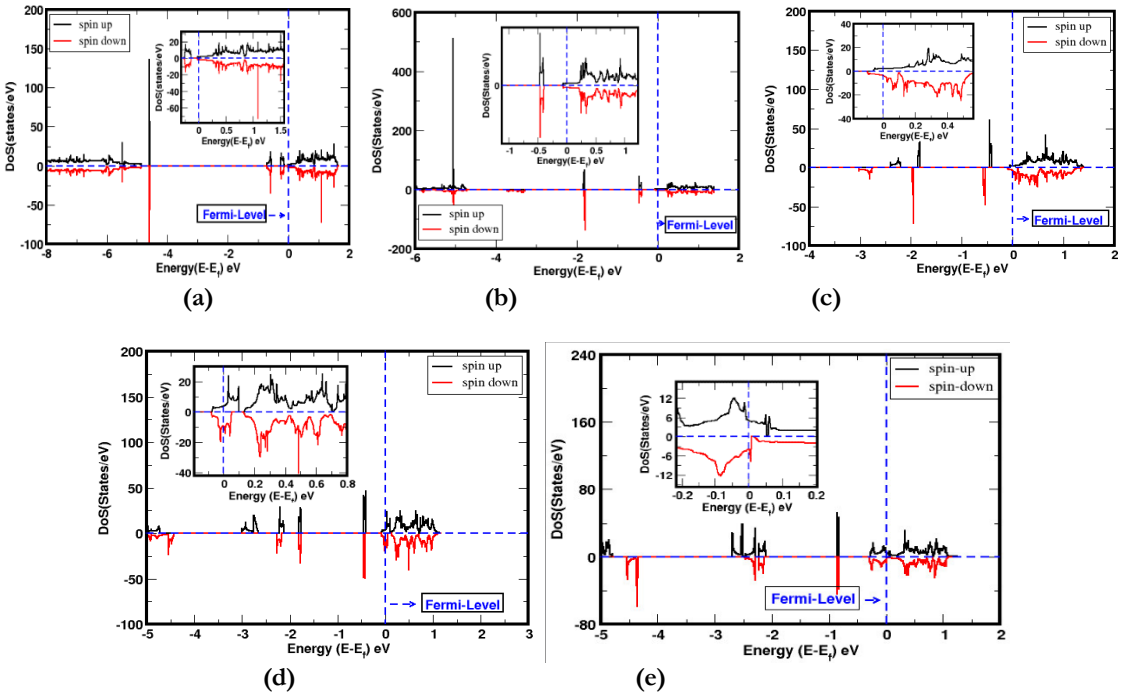

Figure 3. (Colour online) Density of states (DOS) plots of; (a) (4×4) supercell structure of w-hBN material, (b) (4×4) supercell structure of w-1B-hBN material, (c) (4×4) supercell structure of w-1N-hBN material, (d) (4×4) supercell structure of w-nBN-hBN material, and (e) (4×4) supercell structure of w-aBN-hBN material. The horizontal dot line separates the up and down spin states and vertical dot line represent the fermi energy level which distinguish the valence and conduction band. Inset represents the zoom scale of respective plots.

In DOS plot, vertical dot line represents the Fermi energy level, it separates the electronic bands, and horizontal dot lines distinguish the distributed up-spin and down-spin states of electrons in the orbital of atom

present in the material. We have taken DOS states in y-axis, and corresponding energy level in x-axis. The bandgap energy of w-hBN, w-1B-hBN, w-1N-hBN, w-nBN-hBN, & w-aBN-hBN materials have values 3.93 eV, 2.82 eV, 2.71 eV, 2.02 eV & 2.20 eV respectively. It is confirmed that considered materials have semiconducting properties. It is also predicted that w-1B-hBN is a p-type semiconductor material, while w-hBN, w-1N-hBN, w-nBN-hBN, & w-aBN-hBN are n-type semiconducting materials. Semiconducting materials can be used to produce transistors, integrated logic circuits, signal amplifier, photodetectors, flexible optoelectronic devices, solar cells, photocatalysts and lubricants (Neupane & Adhikari, 2020; Nepal *et al.,* 2024). The estimated Fermi energy (E_f), bandgap energy from band structure calculations (E_{gb}), and bandgap energy from DOS calculations (E_{bd}), and nature of materials of w-hBN, w-1B-hBN, w-1N- hBN, w-nBN-hBN & w-aBN-hBN materials are presented in Table 2.

Table 2. Estimated Fermi energy (E_f), bandgap energy from band structure calculations (E_{gb}), and bandgap energy from DOS calculations (E_{bd}), and nature of materials of w-hBN, w-1B-hBN, w-1N- hBN , w-nBN-hBN & w-aBN-hBN materials.

Materials	E_f (eV)	E_{gb} (eV)	E_{gd} (eV)
w-hBN	-1.49	3.96	3.93
w-1B-hBN	-4.82	2.89	2.82
w-1N-hBN	-2.64	2.72	2.71
w-nBN-hBN	-3.38	2.04	2.02
w-aBN-hBN	-3.28	2.30	2.20

Magnetic Properties

We have calculated the magnetic moment of material in order to examine its magnetic properties. In this work, we have used the DOS and partial density of states (PDOS) plots of the materials to compute their magnetic moments. Unpaired electron spins in the atomic orbitals give rise to a material's magnetic properties. They are studied by analyzing material's DOS and PDOS plots. From DOS plot, it is found that up and down spin states of electrons in the orbital of atoms present in the materials are either symmetrically or asymmetrically distributed around the Fermi energy level. Based on the up and down spin states distribution, we can predict that materials have magnetic or non-magnetic properties. The detail calculations of magnetic moment given by individual electronic orbitals of atom present in the materials are determined by the analysis of their PDOS plot (Neupane & Adhikari, 2020). DOS & PDOS plots of w-hBN, w-1B-hBN, w-1N-hBN, w-nBN-hBN, & w-aBN-hBN materials are given in Fig. 3(a-e), and Fig. 4(a-e), respectively. It is observed that up and down spin states of electrons in the orbital of atoms present in the materials are symmetrically distributed around the Fermi energy level in DOS & PDOS plots of w-hBN material, which are shown in Figs. 3(a) and 4(a), respectively. Total magnetic moment of value 0.00 μ_B/cell is given by the distributed up and down spin states in the individual orbital of atom present in the materials (given in Table 3). Hence, w-hBN has non-magnetic properties. We have examined the magnetic moment of w-1B-hBN, w-1N-hBN, w-nBN-hBN, & w-aBN-hBN materials. Up and down spin states of electrons in the orbital of atoms present in w-1B-hBN are asymmetrically distributed around the Fermi energy level in DOS plot, is shown in Fig. 3(b), hence it has magnetic properties. The magnetic moment given by up and down spin states of electrons in the individual orbital of atoms present in material are estimated from the PDOS plot of w-1B-hBN, as illustrated in Fig. 4(b). 2p & 2s orbitals of N atoms respectively contributed 1.80 μ_B/cell & 0.21 μ_B/cell values of magnetic moment in the material. Similarly, -0.13 μ_B/cell & -0.02 μ_B/cell magnetic moment are generated by 2p & 2s orbitals of B atoms in the material. 2s & 2p orbitals of O atom, and 1s orbital of H atoms have no contribution for the production of magnetic moments in the material. Total magnetic moment developed in w-1B-hBN material is estimated to be 1.86 μ_B/cell, hence, w-1B-hBN has magnetic properties. 2p & 2s orbitals of N atoms have a dominant role for the production of magnetic moments than other orbitals of B atoms in the structure. We have predicted the magnetic properties in w-1N-hBN by the examination of its DOS & PDOS plots. In both plots, up and down spin states of electrons are asymmetrically distributed around the Fermi energy level, which reflects that it has magnetic properties. Total magnetic moment -1.00 μ_B/cell is obtained due to the major contribution of magnetic moment of value -0.83 μ_B/cell is given by 2p orbital of B atoms in the material. We have also estimated the magnetic moment given by 2s orbital of B atoms, and 2p orbital of N atoms in the material. They are found to be -0.04 μ_B/cell & -0.08 μ_B/cell, respectively. The negative sign of magnetic moment means, down spin states have more significant contribution for the production of magnetic moment than up spin states in the material. In addition, we have predicted the magnetic properties of w-nBN-hBN & w-aBN-hBN materials by the analysis of their DOS & PDOS plots. DOS & PDOS plots of w-nBN-hBN material are depicted in Figs. 3(d) and 4(d), respectively. It is seen that up and down spin states of electrons are asymmetrically distributed around the Fermi energy level in both plots, hence w-nBN-hBN has magnetic properties. Total magnetic moment -2.00 μ_B/cell of w-nBN-hBN is determined, which is due to the dominant contribution of magnetic moment -1.80 μ_B/cell of 2p orbital of N atoms & -0.27 μ_B/cell of 2s orbital of N atoms in the material. The negative value of magnetic

moment implies that, down spin states of electrons in the orbital of atoms have more contribution than the up spin states of electrons in the orbital of atoms present in the material.

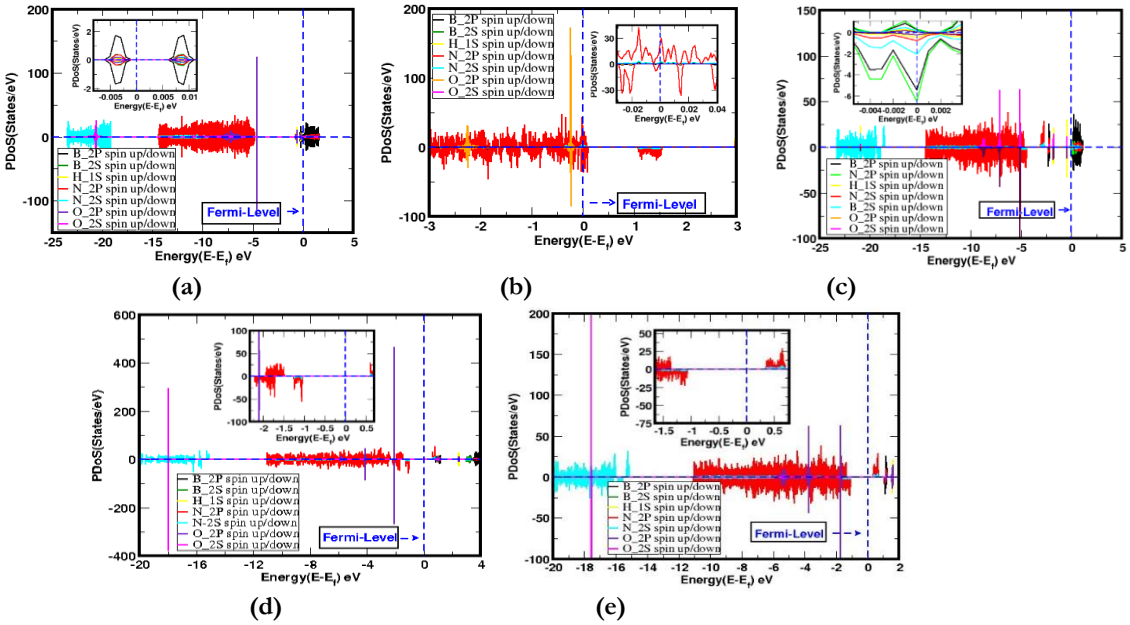

Figure 4. (Color online) Partial density of states (PDOS) plots of; (a) (4×4) supercell structure of w-hBN material, (b) (4×4) supercell structure of w-1B-hBN material, (c) (4×4) supercell structure of w-1N-hBN material, (d) (4×4) supercell structure of w-nBN-hBN material, and (e) (4×4) supercell structure of w-aBN-hBN material. The horizontal dot line separates the up and down spin states and vertical dot line represents the Fermi energy level which distinguish the valence and conduction band. Inset represents the zoom scale of respective plots.

Similarly, we have examined magnetic properties of w-aBN-hBN material through its DOS & PDOS plots, are shown in Figs. 3(e) and 4(e), respectively. It is observed that distributed up and down spin states of electrons are asymmetric around the Fermi energy level. It means, unpaired spin states are available in the material, which generate magnetic moments. Total magnetic moment of w-aBN-hBN is found to be -2.00 μ_B/cell, which is the sum of magnetic moment given by 2p and 2s orbitals of B atoms of values 0.09 μ_B/cell and 0.01 μ_B/cell, and 2p and 2s orbitals of N atoms of values -1.80 μ_B/cell and -0.30 μ_B/cell, respectively. The contribution of magnetic moment given by up and down spin states in the individual orbital of atoms present in w-hBN, w-1B-hBN, w-1N-hBN, w-nBN-hBN and w-aBN-hBN materials are given in Table 3. Magnetic materials can be used in the fields of biomedicine, molecular biology, biochemistry, diagnosis, catalysis, nano electronic devices and various other industrial applications (Neupane & Adhikari, 2020; Paudel *et al.,* 2023).

Table 3. Total magnetic moment (μ) is given by up and down spin states of electrons in the individual orbitals of atoms present in the w-hBN, w-1B-hBN, w-1N-hBN, w-nBN-hBN & w-aBN-hBN materials.

Material's orbital	w-hBN	w-1B-hBN	w-1N-hBN	w-nBN-hBN	w-aBN-hBN
μ of 2p of B atoms (μ_B/cell)	0.00	-0.13	-0.83	0.07	0.09
μ of 2s of B atoms (μ_B/cell)	0.00	-0.02	-0.04	0.00	0.01
μ of 2p of N atoms (μ_B/cell)	0.00	1.80	-0.08	-1.80	-1.80
μ of 2s of N atoms (μ_B/cell)	0.00	0.21	0.00	-0.27	-0.30
μ of 2p of O atom (μ_B/cell)	0.00	0.00	-0.03	0.00	0.00
μ of 2s of O atom (μ_B/cell)	0.00	0.00	-0.02	0.00	-0.00
μ of 1s of H atoms (μ_B/cell)	0.00	0.00	0.00	0.00	0.00
Total (μ_T) μ_B/cell	0.00	1.86	-1.00	-2.00	-2.00

CONCLUSIONS

In this work, we have studied the structural, electronic, and magnetic properties of w-hBN, w-1B-hBN, w-1N-hBN, w-nBN-hBN and w-aBN-hBN materials by using DFT method through the computational tool Quantum ESPRESSO. For the study of structural properties, we have estimated the minimum ground state energy, bond length, bond angles, water adsorption energies of materials, and found that all considered materials are stable. We have investigated the electronic properties of mentioned materials by the analysis of their band structures and density of states (DOS) plots. It is found

that w-1B-hBN is a p-type semiconducting material, while w-hBN, w-1N-hBN, w-nBN-hBN and w-aBN-hBN are n-type semiconducting materials. Bandgap energy of w-hBN, w-1B-hBN, w-1N-hBN, w-nBN-hBN and w-aBN-hBN have values 3.96 eV, 2.89 eV, 2.72 eV, 2.04 eV and 2.30 eV, respectively, obtained from band structure calculations, and 3.93 eV, 2.82 eV, 2.71 eV, 2.02 eV and 2.20 eV, respectively estimated, from DOS plots. The magnetic properties of considered materials are calculated through their DOS, and partial density states (PDOS) plots. It is found that w-hBN is a non-magnetic material, and w-1B-hBN, w-1N-hBN, w-nBN-hBN and w-aBN-hBN materials have magnetic properties. The estimated magnetic moment of w-1B-hBN, w-1N-hBN, w-nBN-hBN and w-aBN-hBN materials have values 1.86 μ_B/cell, -1.00 μ_B/cell, -2.00 μ_B/cell and -2.00 μ_B/cell, respectively. They are obtained due to the unpaired arrangement of spin states of electrons in the individual orbital of atoms present in the material. It is found that non-magnetic pristine h-BN material changes into magnetic material due to the effect of adsorbed water on the defected h-BN. The magnetic properties are tuned due to the effect of adsorption molecules on defected systems.

ACKNOWLEDGEMENTS

Authors greatly appreciated the Condensed Matter Research Lab, CDP, TU, Kirtipur Nepal for the computational facilities. The authors are especially grateful to Prof. Dr. Narayan Prasad Adhikari, for his kind suggestions and help.

AUTHOR CONTRIBUTIONS

SA, GP, MN, DO & OSR: Generated the data and prepared the first draft of manuscript; HKN: supervised this work and prepared the final form of manuscript.

CONFLICT OF INTEREST

There is no conflict of interest in authors

DATA AVAILABILITY

The data that is used to create figures and tables are available upon request to the corresponding author.

REFERENCES

Bhimanapati, G.R., Lin, Z., Meunier, V., Jung, Y., Cha, J., Das, S., Xiao, D., Son, Y., Strano, M.S., Cooper, V.R., et al. (2015). Recent advances in two-dimensional materials beyond graphene. *ACS Nano*, *9*(12), 11509–11539.

Butler, S.Z., Hollen, S.M., Cao, L., Cui, Y., Gupta, J.A., Gutiérrez, H.R., Heinz, T.F., Hong, S.S., Huang, J., Ismach, A.F., et al. (2013). Progress, challenges, and opportunities in two-dimensional materials beyond graphene. *ACS Nano*, *7*(4), 2898–2926.

Giannozzi, P., Baroni, S., Bonini, N., Calandra, M., Car, R., Cavazzoni, C., & Dal Corso, A. (2009). Quantum ESPRESSO: modular and open-source software Project for quantum simulations of materials. *Journal of Physics: Condensed Matter, 21*(39), 395502.

He, W., Kong, L., Zhao, W., & Yu, P. (2022). Atomically thin 2D van der Waals magnetic materials: Fabrications, structure, magnetic properties and applications. *Coatings*, *12*(2), 122.

Head, J.D., & Zerner, M.C. (1985). A Broyden-Fletcher-Goldfarb-Shanno optimization procedure for molecular geometries. *Chemical Physics Letters*, *122*(3), 264–270.

Kohn, W., & Sham, L.J. (1965). Self-consistent equations including exchange and correlation effects. *Physical Review*, *140*(4A), A1133–A1138.

Kokalj, A. (2003). Computer graphics and graphical user interfaces as tools in simulations of matter at the atomic scale. *Computational Materials Science*, *28*(2), 155–168.

Kresse, G., & Joubert, D. (1999). From ultrasoft pseudopotentials to the projector augmented-wave method. *Physical Review B*, *59*(3), 1758.

Liu, Y.J., Gao, B., Xu, D., Wang, H.M., & Zhao, J.-X. (2014). Theoretical study on Si-doped hexagonal boron nitride (h-BN) sheet: Electronic, magnetic properties, and reactivity. *Physical Letters* A, *378*(40), 2989–2994.

Mali, K.S., Greenwood, J., Adisoejoso, J., Phillipson, R., & De Feyter, S. (2015). Nanostructuring graphene for controlled and reproducible functionalization. *Nanoscale*, *7*(5), 1566–1585.

Marzari, N., Vanderbilt, D., De Vita, A., & Payne, M.C. (1999). Thermal Contraction and disordering of the Al (110) surface. *Physical Review Letters, 82*(16), 3296.

Nepal, M., Paudel, G., Aryal, S., Devkota, A., & Neupane, H.K. (2024). Adsorption of water on vacancy defective h-BN bilayer at B and N sites: First-principles calculation. *Bibechana*, *21*(2), 129-141.

Neupane, H.K., & Adhikari, N.P. (2020). Structure, electronic and magnetic properties of 2D Graphene-Molybdenum diSulphide (G-MoS_2) Heterostructure (HS) with vacancy defects at Mo sites. *Computational Condensed Matter*, *24*, e00489.

Neupane, H.K., & Adhikari, N.P. (2021a). Effect of vacancy defects in 2D vdW graphene/h-BN heterostructure: First-principles study. *AIP Advances*, *11*(8), 085218.

Neupane, H.K., & Adhikari, N.P. (2021b). First-principles study of structure, electronic, and magnetic properties of C sites vacancy defects in water adsorbed graphene/MoS_2 van der Waals heterostructures. *Journal of Molecular Modeling*, *27*(3), 82.

Neupane, H.K., & Adhikari, N.P. (2022). Adsorption of water on C sites vacancy defected graphene/h-BN: First-principles study. *Journal of Molecular Modeling*, *28*(4), 107.

Neupane, H.K., & Adhikari, N.P. (2020). Tuning structural, electronic, and magnetic properties of C sites vacancy defects in graphene/MoS_2 van der Waals heterostructure materials: A first-principles study. *Advances in Condensed Matter Physics*, *2020*(1), 8850701.

Neupane, H.K., & Adhikari, N.P. (2022). Adsorption of water on C sites vacancy defected graphene/h-BN: First-principles study. *Journal of Molecular Modeling*, *28*(4), 107.

Neupane, H.K., & Adhikari, N.P. (2021). First-Principles Study of Vacancy and Impurities Defects in Graphene. *Amrit Research Journal*, *2*(01), 93-102.

Novoselov, K.S., Mishchenko, A., Carvalho, A., & Castro Neto, A. (2016). 2D materials and van der Waals heterostructures. *Science*, *353*(6298), aac9439.

Oli, D. (2024). *Adsorption of HCN and H_2S over ZnO and Al-ZnO monolayer* [M.Sc. Thesis]. Amrit Campus.

Patra, A.S., Chauhan, M.S., Keene, S., Gogoi, G., Reddy, K.A., Ardo, S., Prasad, D.L., & Qureshi, M. (2018). Combined experimental and theoretical insights into the synergistic effect of cerium doping and Oxygen vacancies in BaZrO3- δ Hollow nanospheres for efficient photocatalytic hydrogen production. *The Journal of Physical Chemistry C*, *123*(1), 233–249.

Paudel, G., Nepal, M., Aryal, S., Devkota, A., & Neupane, H. (2023). Effect of water adsorption on bilayer h-BN: First-principles study. *Journal of Nepal Physical Society*, *9*(2), 56–62.

Pierucci, D., Zribi, J., Henck, H., Chaste, J., Silly, M.G., Bertran, F., Le Fevre, P., Gil, B., Summerfield, A., Beton, P.H., et al. (2018). Van der Waals epitaxy of two-dimensional single-layer h-BN on graphite by molecular beam epitaxy: Electronic properties and band structure. *Applied Physics Letters*, *112*(25), 253102.

Perdew, J.P., Burke, K., & Ernzerhof, M. (1996). Generalized gradient approximation made simple, *Physical Review Letters, 77*(18), 3865.

Ren, G., Han, W., Deng, Y., Wu, W., Li, Z., Guo, J., Bao, H., Liu, C., & Guo, W. (2021). Strategies of modifying spiro-OMeTAD materials for perovskite solar cells: A review. *Journal of Materials Chemistry A*, *9*(8), 4589–4625.

Turner, P. (2005). XMGRACE, Version 5.1. 19. *Center for Coastal and Land-Margin Research, Oregon Graduate Institute of Science and Technology, Beaverton, OR*, *2*.

Uddin, M.M., Kabir, M.H., Ali, M.A., Hossain, M.M., Khandaker, M.U., Mandal, S., Arifutzzaman, A., & Jana, D. (2023). Graphene-like emerging 2D materials: Recent progress, challenges and future outlook. *RSC Advances*, *13*(47), 33336–33375.

Vu, T.V., Hieu, N.V., Phuc, H.V., Hieu, N.N., Bui, H. D., Idrees, M., Amin, B., & Nguyen, C.V. (2020). Graphene/WSeTe van der Waals heterostructure: Controllable electronic properties and Schottky barrier via interlayer coupling and electric field. *Applied Surface Science*, *507*, 145036.

Xu, M., Liang, T., Shi, M., & Chen, H. (2013). Graphene-like two-dimensional materials. *Chemical Reviews*, *113*(5), 3766–3798.

Zhang, J., Liu, X., Neri, G., & Pinna, N. (2016). Nanostructured materials for room-temperature gas sensors. *Advanced Materials*, *28*(5), 795–831.

Zhang, X., & Zhang, L. (2010). Electronic and band structure tuning of ternary semiconductor photocatalysts by self doping: The case of BiOI. *The Journal of Physical Chemistry C*, *114*(42), 18198–18206.